Stationary solutions for the $1 + 1$ nonlinear Schrödinger equation modeling attractive Bose-Einstein condensates in small potentials

Kristina Mallory and Robert A. Van Gorder[*]

Department of Mathematics, University of Central Florida, Orlando, Florida 32816-1364, USA

Stationary solutions for the $1 + 1$ cubic nonlinear Schrödinger equation (NLS) modeling attractive Bose-Einstein condensates (BECs) in a small potential are obtained via a form of nonlinear perturbation. The focus here is on perturbations to the bright soliton solutions due to small potentials which either confine or repel the BECs: under arbitrary piecewise continuous potentials, we obtain the general representation for the perturbation theory of the bright solitons. Importantly, we do not need to assume that the nonlinearity is small, as we perform a sort of nonlinear perturbation by allowing the zeroth-order perturbation term to be governed by a nonlinear equation. This is useful, in that it allows us to consider perturbations of bright solitons of arbitrary size. In some cases, exact solutions can be recovered, and these agree with known results from the literature. Several special cases are considered which involve confining potentials of specific relevance to BECs. We make several observations on the influence of the small potentials on the behavior of the perturbed bright solitons. The results demonstrate the difference between perturbed bright solitons in the attractive NLS and those results found in the repulsive NLS for dark solitons, as discussed by Mallory and Van Gorder, [Phys. Rev. E **88**, 013205 (2013)]. Extension of these results to more spatial dimensions is mentioned.

I. INTRODUCTION

The cubic form of the nonlinear Schrödinger equation (NLS) has been used to model the dilute-gas Bose-Einstein condensate (BEC) in the quasi-one-dimensional regime [1]. The scalar potential in the NLS can be used to model a trap when dealing with applications to BECs. The actual application will dictate the class of confining potentials employed [2], and indeed a wide variety of scalar potentials have appeared in the literature. Exact NLS solutions have been reported for specific potentials, and these include the Kronig-Penney potential [3] and the Jacobi sn potential [4]. Exact solutions for the latter case took the form of Jacobi elliptic functions of type sn, cn, or dn, depending on the values of the model parameter. The Jacobi elliptic functions have trigonometric functions as degenerate limits, and in the limit of a space-periodic potential, those solutions are one possible description of a dilute-gas Bose-Einstein condensate trapped in a standing light wave. Note that BECs trapped in a standing light wave have been used to study or have been proposed to study multiple phenomena such as phase coherence [5], matter-wave diffraction [6], quantum logic [7], and matter-wave transport [8].

Stationary solutions, or ground state solutions, for the NLS with various potentials are frequently considered. Concerning potentials relevant to BECs, stationary solutions to the one-dimensional NLS under box and periodic boundary conditions were considered analytically for the repulsive [9] and attractive [10] cases, while BECs in a ring-shaped trap with a nonlinear double-well potential have also been considered [11]. PT-symmetric BEC solutions in a δ-function double-well potential have been studied [12]. Multiwell potentials make useful BEC traps in a variety of physical scenarios [13].

Let $V(x)$ be a potential function which has been normalized so that $\max V(x) = 1$. Then, the $n + 1$ cubic nonlinear Schrödinger equation (NLS) (also referred to as the Gross-Pitaevskii model in some literature [14]) with small potential reads as

$$i\hbar\Psi_t = \left(-\frac{\hbar^2}{2m}\nabla^2 + \epsilon V(\mathbf{r}) + g|\Psi|^2\right)\Psi. \qquad (1)$$

For our interests, we shall be concerned with the $1 + 1$ model

$$i\hbar\Psi_t = -\frac{\hbar^2}{2m}\Psi_{xx} + \epsilon V(x)\Psi + g|\Psi|^2\Psi. \qquad (2)$$

When $g > 0$, we have the repulsive case. General perturbation results (of the type we seek here) were recently given in Ref. [15] for the repulsive case. The repulsive case holds dark solitons as one special solution. In this paper, we shall be interested in perturbation results for the attractive case ($g < 0$). This latter case will hold bright solitons as a special class of solutions.

If $\epsilon = 0$ and $g > 0$, we have the free particle potential and we recover an exact solution. Under further assumptions, this exact solution reduces to the standard dark soliton solution. For a constant potential $V(x) = \lambda$, we have a mass-shifted variant of the zero-potential case. Since the $\epsilon = 0$ case results in Jacobi elliptic function solutions, Ref. [4] considered Jacobi elliptic functions as possible trapping potentials. Exact solutions involving Jacobi elliptic functions [16] were then obtained. Other potentials were considered in Ref. [4], where a mix of analytical and numerical results were given. The above special solutions can be seen in a broader context, if one considers general potential functions $V(x)$. A perturbation method for arbitrary potentials has been proposed [15] for repulsive BECs. A number of known exact or numerical solutions which were obtained as special cases in Ref. [4] were then recovered easily in Ref. [15].

In this paper, the general perturbation analysis of [15] will be considered in the context of attractive BECs. The

---

*Corresponding author: rav@knights.ucf.edu

analysis is similar, yet the results will be distinct, owing to the qualitative differences between attractive and repulsive BECs. We shall develop a general perturbation theory of stationary solutions to the $1 + 1$ model (2) under $g < 0$ for small yet arbitrary potential functions. The lowest order term will be governed by a nonlinear ordinary differential equation (ODE), as opposed to a linear ODE, permitting us to consider perturbations about bright solitons and other nonlinear waves. In order to demonstrate the results concretely, we consider a diverse section of small potentials. Exact solutions present in the literature can easily be found in this framework. For other situations, where solutions can not be found in exact closed form, the first-order perturbation terms are obtained. Examples of cases we consider include the δ function potential, the linear potential, the harmonic potential, the Coulomb potential, the Morse potential, and the quantum pendulum potential since these have been shown to be of physical relevance. Unlike in Ref. [15], we were able to ascertain the qualitative influence of such potentials on perturbations to the bright soliton BECs.

The approach taken here permits very general forms of the potential function, so for sufficiently well-behaved functions $V(x)$, we are able to calculate the first-order perturbation theory for the stationary solutions to the model (2) given potentials of the form $\epsilon V(x)$. As we consider a type of nonlinear perturbation (the zeroth-order term is governed by a nonlinear differential equation), we need not assume a small amplitude solution, requiring only that the higher-order corrections are small. As such, there are no unnatural size restrictions on the bright solitons. Therefore, the results maintain physical relevance under a very wide variety of small potentials.

II. STATIONARY SOLUTION AND ORDER-ZERO PERTURBATION THEORY

We begin by introducing the stationary solution

$$\Psi(x,t) = \frac{\sqrt{2}\hbar}{\sqrt{|g|m}} \exp\left(i\frac{\hbar}{m}t\right)\psi(x), \qquad (3)$$

which utilizes an exponential of the form $\exp(+it)$, as opposed to the exponential $\exp(-it)$, which was taken in Ref. [15] for the case of repulsive BECs. This assumption reduces (2) to the eigenvalue problem

$$\psi'' = \psi - 2\psi^3 + \epsilon U(x)\psi, \qquad (4)$$

where we define the nondimensional potential U by

$$U(x) = \frac{m}{\hbar^2}V(x). \qquad (5)$$

Note that we may obtain (4) from a number of different transformations. Assuming a general stationary solution of the form

$$\Psi(x,t) = \sqrt{2}\alpha e^{i\beta t}\psi(X), \quad X = \gamma x \qquad (6)$$

we reduce (2) to

$$\frac{d^2\psi}{dX^2} = \psi - 2\psi^3 + \epsilon U(X)\psi, \qquad (7)$$

provided that

$$\beta = \alpha^2|g|^2, \quad \gamma = \frac{\sqrt{2m}}{|\alpha||g|\hbar}, \qquad (8)$$

where

$$U(X) = \frac{1}{\alpha^2|g|^2}V\left(\frac{X}{\gamma}\right). \qquad (9)$$

This gives us a family of stationary solutions, parametrized by the scaling factor α, which read as

$$\Psi(x,t) = \sqrt{2}\alpha \exp(i\alpha^2|g|^2)\psi\left(\frac{\sqrt{2m}}{|\alpha||g|\hbar}x\right). \qquad (10)$$

Therefore, to study any of these types of stationary solutions, it is sufficiently general to study the behavior of solutions to (4).

Of course, since (4) is nonlinear and has an arbitrary potential function, exact solutions are not possible. Still, analytical results will be desirable, so it is natural to study analytical properties of the stationary solutions in the presence of small potentials, that is, $\epsilon \ll 1$. If we consider a perturbation solution of the form

$$\psi(x) = \psi_0(x) + \epsilon\psi_1(x) + \epsilon^2\psi_2(x) + \cdots, \qquad (11)$$

then we may obtain the perturbative stationary solution to the $1 + 1$ GP equation

$$\begin{aligned}
\Psi(x,t) &= \Psi_0(x,t) + \epsilon\Psi_1(x,t) + \epsilon^2\Psi_2(x,t) + \cdots \\
&= \frac{\sqrt{2}\hbar}{\sqrt{|g|m}} \exp\left(i\frac{\hbar}{2m}t\right) \\
&\quad \times [\psi_0(x) + \epsilon\psi_1(x) + \epsilon^2\psi_2(x) + \cdots]. \quad (12)
\end{aligned}$$

Now, utilizing the perturbation solution (11), we see that $\psi_0(x)$ satisfies

$$\psi_0'' = \psi_0 - 2\psi_0^3. \qquad (13)$$

Thus, our solution to (13), with the assumed initial conditions $\psi_0(0) = 1$ and $\psi_0'(0) = 0$, reads as

$$\psi_0(x) = \mathrm{sech}(x). \qquad (14)$$

This represents the bright soliton solution. Our solutions, therefore, will become perturbations around this bright soliton solution. The comparable dark soliton solution, and the general perturbation theory thereof, was obtained in the case of repulsive BECs [15].

III. PERTURBATION SOLUTIONS FOR GENERAL POTENTIALS

Let us now compute the higher-order terms in the perturbation expansion (11) for the general potential $U(x)$. Notice we will utilize $\psi_0'(x)$ as the function given by

$$\psi_0'(x) = -\mathrm{sech}(x)\tanh(x), \qquad (15)$$

where $\psi_0(x)$ is our previously determined function (14). Placing (11) into our Eq. (4), we obtain $\psi_1(x)$ via the linear differential equation represented in the first-order term in ϵ, namely,

$$\psi_1''(x) + [6\,\mathrm{sech}^2(x) - 1]\psi_1(x) = U(x)\mathrm{sech}(x). \qquad (16)$$

Satisfying $\psi_1(0) = 0$ and $\psi_1'(0) = 0$, our first-order term becomes

$$
\begin{aligned}
\psi_1(x) = \frac{1}{2} \int_0^x U(y)\psi_0(y) \\
\times \{\psi_0'(x)[\cosh(y) - 3y\psi_0'(y) - 3\psi_0(y)] \\
- \psi_0'(y)[\cosh(x) - 3x\psi_0'(x) - 3\psi_0(x)]\} dy. \quad (17)
\end{aligned}
$$

Now, in a similar manner, we may obtain our second-order solution $\psi_2(x)$ by solving the relevant ODE subject to $\psi_2(0) = 0$ and $\psi_2'(0) = 0$, which gives

$$
\begin{aligned}
\psi_2(x) = \frac{1}{2} \int_0^x \left[U(y)\psi_1(y) - 6\psi_1^2(y)\psi_0(y) \right] \\
\times \{\psi_0'(x)[\cosh(y) - 3y\psi_0'(y) - 3\psi_0(y)] \\
- \psi_0'(y)[\cosh(x) - 3x\psi_0'(x) - 3\psi_0(x)]\} dy. \quad (18)
\end{aligned}
$$

With this, we have determined the second-order perturbation theory for the stationary solution under a general potential $U(x)$. In the next section, we shall utilize our general solution to consider stationary solutions under specific forms of $U(x)$ and to explore the resulting solutions.

It should be mentioned that the perturbation results here involve perturbation about sech-type bright solitons. However, it is possible to conduct such a general analysis using Jacobi cn-type solutions. This was done using Jacobi sn-type solutions in Ref. [15]. The cn solutions are a natural generalization of the sech solitons. As we shall see later, in some situations the perturbation of sech solitons results in space-periodic solutions over part of the domain. Such space-periodic solutions can be described in terms of Jacobi cn functions.

The perturbation results here are useful for two main reasons. First of all, note that there is no amplitude restriction on the amplitude of the order-zero perturbation term (the pure bright soliton). So, the results present here are not limited by the amplitude of the original (unperturbed) solutions, but rather by the size of the excitations. This is highly relevant since oftentimes a nonsmall solution will experience small perturbation (in our model, the perturbation is due to a small potential). The reason this is possible lies in the form of the order-zero equation. Indeed, the order-zero equation is actually the NLS without a potential. Since this model is exactly solvable, one obtains an exact nonlinear wave solution. As the potential is a perturbation of this exactly solvable model, we are able to preserve properties of the original nonlinear wave solution.

Second, the method here is robust for rather arbitrary forms of the potential function $U(x)$. The restriction is that the total potential $\epsilon U(x)$ is small, and must be sufficiently well behaved. In particular, the integrals discussed in this section must exist for our choice of $U(x)$. However, this is not a particularly strong condition. Indeed, piecewise continuous $U(x)$ will satisfy this requirement, and such $U(x)$ essentially contain most potentials of physical relevance. However, more poorly behaved potentials can also be included. One such potential would be the delta potential, which we shall study later. Hence, the results obtained here are very general with respect to the types of potential allowed.

IV. SOLUTIONS FOR SPECIFIC POTENTIALS

We now turn our attention toward a number of examples of specific potentials in order to illustrate the method. For such potentials, we demonstrate the analytical construction of the perturbation solutions for the bright soliton case. For all perturbation solutions considered, we provide plots of the density $|\Psi(x,t)|^2 = |\psi(x)|^2$ in order to demonstrate the influence of each potential on the obtained solutions. As will be remarked later, the perturbation results are in agreement with numerical simulations, for sufficiently small ϵ. We begin with several exact solutions, in order to give a complete classification of perturbations of bright solitons due to small potentials.

A. Free particle

Note that the free particle solution, corresponding to $U(x) \equiv 0$, is exactly determined by $\psi_0(x)$. As such,

$$
\Psi(x,t) = \frac{\sqrt{2}\hbar}{\sqrt{|g|m}} \exp\left(i\frac{\hbar}{2m}t\right) \text{sech}(x) \quad (19)
$$

is an exact bright soliton solution for the free particle.

B. Constant potential

Let us consider the constant potential $U(x) = \lambda$. With this potential, (1) models a vortex filament in an almost ideal Bose gas [14]. Now, notice that when we employ the potential $U(x) = \lambda$, our Eq. (4) may be rewritten as

$$
\psi'' = (1 + \epsilon\lambda)\psi - 2\psi^3, \quad (20)
$$

which is merely a rescaling of the equation solved in the previous section for the free particle. This leads us to then consider a rescaling of the corresponding solution of the form $\psi(x) = a \, \text{sech}(bx)$. Plugging this into (20) gives the equation

$$
b^2\psi'' = (1 + \epsilon\lambda)\psi - 2a^2\psi^3, \quad (21)
$$

so that $a = b = \sqrt{1 + \epsilon\lambda}$ lets us utilize the solution

$$
\psi(x) = \sqrt{1 + \epsilon\lambda} \, \text{sech}(\sqrt{1 + \epsilon\lambda}\, x) \quad (22)
$$

as an exact solution for the case of a constant potential. We then have the exact solution for the wave function given by

$$
\Psi(x,t) = \frac{\hbar\sqrt{2(1 + \epsilon\lambda)}}{\sqrt{|g|m}} \exp\left(i\frac{\hbar}{2m}t\right) \text{sech}(\sqrt{1 + \epsilon\lambda}x). \quad (23)
$$

C. Delta potential

The δ potential is given by $U(x) = \lambda\delta(x - x_0)$, where δ denotes the Dirac delta function, $\lambda \in \mathbb{R}$, and $x_0 \in \mathbb{R}$ is a constant. This potential arises in some applications [17]. Note also that the results we obtain here are similar for the double delta potential [18]. Note that the quantum Hall effect of bosons interacting through a delta potential has been considered previously [19].

Notice that for the delta potential, we may construct an exact solution which is continuous. However, the derivative of such a solution will necessarily have a jump discontinuity, so such a solution is a weak solution: it satisfies the differential equation, but there is a loss of regularity of the derivatives.

This makes complete sense when one considers the fact that the delta potential causes an impulse in the second derivative, and hence a jump in the first derivative.

Take $U(x) = \lambda\delta(x - x_0)$ and integrate over (4). Assume a solution with a branch $x < x_0$ and a branch for $x > x_0$, say

$$\psi(x) = \begin{cases} \psi_-(x), & x \leqslant x_0 \\ \psi_+(x), & x > x_0. \end{cases} \tag{24}$$

Then, we have

$$\psi_-'^2 = \psi_-^2 - \psi_-^4, \tag{25}$$

when $x \leqslant x_0$, and

$$\psi_+'^2 = \psi_+^2 - \psi_+^4 + 2\epsilon\lambda\psi_+(x_0)\psi_+'(x_0), \tag{26}$$

when $x > x_0$. Clearly, $\psi_-(x) = \text{sech}(x)$ on $-\infty < x \leqslant x_0$. For a continuous solution, we require $\psi_+(x_0) = \psi_-(x_0) = \text{sech}(x_0)$. The second initial condition satisfies $\psi_+'^2(x_0) = \psi_+^2(x_0) - \psi_+^4(x_0) + 2\epsilon\lambda\psi_+(x_0)\psi_+'(x_0) = \psi_-'^2(x_0) + 2\epsilon\lambda\psi_-(x_0)\psi_-'(x_0)$. Solving for $\psi_+'(x_0)$,

$$\psi_+'(x_0) = \text{sech}(x_0)\{\epsilon\lambda \pm \sqrt{\tanh^2(x_0) + \epsilon^2\lambda^2}\}. \tag{27}$$

In the limit $x_0 \to 0$, we want $\psi_+'(x_0) \to 0$, so we take the $-$ sign, obtaining

$$\psi_+'(x_0) = \mu = \text{sech}(x_0)\{\epsilon\lambda - \sqrt{\tanh^2(x_0) + \epsilon^2\lambda^2}\} < 0, \tag{28}$$

where we define the constant $\mu = \mu(x_0)$ for convenience. If we assume a solution $\psi_+(x) = a_1\text{sn}(a_2x, a_3)$, where sn denotes the Jacobi elliptic function, we obtain the system of algebraic equations $a_1^2 + a_2^2a_3^2 = 0$, $1 + a_2^2(1 + a_3^2) = 0$, $\mu - a_1^2a_2^2 = 0$. We then obtain

$$\psi_+(x) = \frac{\sqrt{2|\mu|}}{\sqrt{1 - \sqrt{1 - 4|\mu|}}}$$
$$\times \text{sn}\left(i\sqrt{\frac{1 - \sqrt{1 - 4|\mu|}}{2}}x, \frac{-2|\mu|}{1 - \sqrt{1 - 4|\mu|}}\right). \tag{29}$$

Interestingly, these solutions oscillate in space. So, the solution has a standard sech-type bright soliton profile up until it hits $x = x_0$, past which the sech-wave fractures into a space-periodic structure governed by a Jacobi sn function. Note that in the limit $x_0 \to 0$, $\mu \to 0$ and $\frac{-2|\mu|}{1 - \sqrt{1 - 4|\mu|}} \to -1$, which causes the sn function to reduce to a sech function. So, we recover the solution $\psi(x) = \text{sech}(x)$ in the $x_0 \to 0$ limit.

For the present example, we were lucky to be able to obtain an exact piecewise solution. For general potential functions $U(x)$, exact solutions are not possible. However, the analytical techniques derived in Sec. III can be applied to such situations. As we shall see in later examples, the sech-type bright soliton solutions are frequently found to decay into Jacobi sn-type waves, which exhibit a type of damped oscillation as they decay to zero as $x \to \pm\infty$. In the present example, however, the solution on $x < x_0$ is of sech type, while the solution on $x > x_0$ is always a Jacobi sn wave with no damping. So, the sn waveform is maintained asymptotically as $x \to \infty$.

This is interesting in the context of the results of [9,10,15]. While we have considered the perturbation of a sech-type bright soliton due to a small potential, the perturbation resulted in a space-periodic solution to the right of $x = x_0$. Such space-periodic solutions have been discussed before [9,10,15]. Indeed, in the repulsive BEC, it was shown that the dark soliton solutions can be perturbed in such a way that space-periodic solutions result. It was also shown that Jacobi sn and cn waves were more general than the tanh-type soliton.

In the attractive case, this form of degeneracy due to small perturbations appears to hold true as well. As one perturbs an attractive BEC, with mass centered near the origin, the BEC reconfigures itself so that mass density peaks appear periodically to the right of $x = x_0$ as well as near the origin. For the exact piecewise solution obtained here, these density peaks are equal in amplitude and appear completely periodically (where the period is given by the period of the relevant sn function). However, in later examples (where the potential function takes a different form), the additional mass density peaks decay in size as one moves away from the origin. These solutions therefore preserve an envelope much like the pure bright solitons, with the difference being that mass is not purely monotone decreasing as one moves away from the origin.

D. sech² potential

It is often possible to obtain soliton solutions in the case where the potential itself takes the form of the soliton wave envelope. This was studied previously in the case of elliptic potentials for BECs. It was found that when the potential was the square of a Jacobi elliptic function, exact solutions can be constructed in terms of such a Jacobi elliptic function (not necessarily of the same type). For the dark soliton case, this would be equivalent to studying the tanh potential.

For our purposes, let us assume that $U(x)$ takes the form $U(x) = f(\psi(x))$. We should remark that the elliptic potential cases previously studied used the functional form $f(\psi) = \psi^2$. We find that (4) yields

$$\psi'' = \psi - 2\psi^3 + \epsilon f(\psi)\psi. \tag{30}$$

A first integral for this equation reads as

$$\psi'^2 = \psi^2 - \psi^4 + 2\epsilon\int_{\psi(0)}^{\psi} f(\xi)\xi \, d\xi + C, \tag{31}$$

where C is a constant of motion. If we denote $F(\psi) = 2\int_{\psi(0)}^{\psi} f(\xi)\xi \, d\xi$, then ψ is determined from the implicit relation

$$\pm x = \int_{\psi(0)}^{\psi(x)} \frac{dk}{\sqrt{k^2 - k^4 + \epsilon F(k) + C}}. \tag{32}$$

Under our definition of F, we must have $F(\psi(0)) = 0$, and hence $C = \psi^4(0) - \psi^2(0)$. The study of such solutions defined implicitly by (32) is equivalent to the study of NLS equations with higher-order nonlinearity. For instance, one would want to study NLS equations of the form

$$i\Psi_t = \Psi_{xx} + |\Psi|^2\Psi + \epsilon f(|\Psi|)\Psi \tag{33}$$

in order to deduce the behavior of these solutions. Such an equation accounts for any situation where the potential function U depends strictly on the solution Ψ. In such a case, there are two options: perturbation solutions (truncated after terms of order ϵ) or exact solutions.

In the case where $f(\psi) = \lambda \psi^2$, let us consider the effect on the bright soliton $\psi(x) = \mathrm{sech}(x)$. With this, the explicit form of the potential is $U(x) = \lambda \, \mathrm{sech}^2(x)$, so

$$\psi'' = \psi - 2\psi^3 + \epsilon \lambda \, \mathrm{sech}^2(x)\psi. \qquad (34)$$

The solution can not exactly be $\psi(x) = \mathrm{sech}(x)$, as a simple calculation will show. However, let us introduce a scaling $\psi(x) = \alpha \, \mathrm{sech}(x)$. Then, we have a solution corresponding to $\alpha = \sqrt{1 + \epsilon\lambda/2}$. Hence, when the potential takes the form $U(x) = \lambda \, \mathrm{sech}^2(x)$, we have an exact solution

$$\psi(x) = \sqrt{1 + \frac{\epsilon\lambda}{2}} \, \mathrm{sech}(x). \qquad (35)$$

So, a scaling of the bright soliton is sufficient to pick up the effect of a perturbation due to the small potential of the form $\epsilon\lambda \, \mathrm{sech}^2(x)$. Importantly, this means we can obtain an exact solution for such a potential. Unlike in the case of the delta potential considered above, we keep a sech-type bright soliton solution despite the perturbation. Hence, the stationary states appear stable under perturbations with a potential of the form $\epsilon\lambda \, \mathrm{sech}^2(x)$.

When exact solutions are not possible, we can still consider perturbation solutions. Let us assume ϵ is sufficiently small. From (32), we can write

$$\pm\, x = \int_{\psi(0)}^{\psi(x)} \frac{dk}{\sqrt{k^2 - k^4 + C}}$$
$$- \frac{\epsilon}{2} \int_{\psi(0)}^{\psi(x)} \frac{F(k)\,dk}{[k^2 - k^4 + C]^{3/2}} + O(\epsilon^2). \qquad (36)$$

If we consider the initial condition $\psi(0) = 1$, then $C = 0$ and (32) reduces to

$$\pm\, x = -\int_{\psi(x)}^{1} \frac{dk}{\sqrt{k^2 - k^4}} + \frac{\epsilon}{2} \int_{\psi(x)}^{1} \frac{F(k)\,dk}{[k^2 - k^4]^{3/2}} + O(\epsilon^2). \qquad (37)$$

The first integral is simply equal to $\mathrm{sech}^{-1}[\psi(x)] - \mathrm{sech}^{-1}(1) = \mathrm{sech}^{-1}[\psi(x)]$, hence

$$\pm x = \mathrm{sech}^{-1}[\psi(x)] + \frac{\epsilon}{2} \int_{\psi(x)}^{1} \frac{F(k)\,dk}{[k^2 - k^4]^{3/2}} + O(\epsilon^2). \quad (38)$$

Clearly, when $\epsilon = 0$, we recover the $\psi(x) = \mathrm{sech}(x)$ solution. This gives further indication that the perturbation solutions for potentials which depend on sech [i.e., $U(x) = f(\mathrm{sech}(x))$] should result in perturbation which retains the general form of the unperturbed bright soliton.

E. Exact solutions for sn²-, cn²-, and dn²-type potentials

In the case of sn-, cn-, or dn-type waves, similar results can be obtained. Such results were outlined in the repulsive BEC case [15] for $g > 0$. Some specific applications were given in Refs. [9,10]. In particular, the attractive BECs in a box or periodic potential were described in terms of Jacobi elliptic functions. These results can be obtained through the formulation (30) [or, equivalently, (32)].

In the case where $U(x) = \lambda \, \mathrm{sn}^2(x,k)$, let us consider a solution which attains a maximal value at $x = 0$. Such a solution can be represented by $\psi(x) = A \, \mathrm{cn}(x,k)$. We find that

this solution exists provided $A = 1$ and $2k^2 = 2 + \epsilon\lambda$. So, for the potential

$$U(x) = \lambda \, \mathrm{sn}^2\left(x, \pm\sqrt{1 + \frac{\epsilon\lambda}{2}}\right), \qquad (39)$$

we have the exact solution

$$\psi(x) = \mathrm{cn}\left(x, \pm\sqrt{1 + \frac{\epsilon\lambda}{2}}\right). \qquad (40)$$

In the limit $\epsilon \to 0$, this reduces to $\psi(x) = \mathrm{sech}(x)$.

In the case where $U(x) = \lambda \, \mathrm{cn}^2(x,k)$, we again assume a solution $\psi(x) = A \, \mathrm{cn}(x,k)$. Such a solution exists provided $2A^2 - 2k^2 - \epsilon\lambda = 0$ and $\epsilon\lambda + 2 = 2A^2$. Then, $A = \sqrt{1 + \frac{\epsilon\lambda}{2}}$ and hence $k = \pm 1$. Yet, $\mathrm{cn}(x, \pm 1) = \mathrm{sech}(x)$. So, the potential reduces to that of the type $U(x) = \lambda \, \mathrm{sech}^2(x)$ considered before. We therefore have the solution (35).

In the case where $U(x) = \lambda \, \mathrm{dn}^2(x,k)$, we again find that $k = \pm 1$, hence the dn case also degenerates into the case of a sech^2 potential. As such, we again have the solution (35).

Interestingly, we only obtained a new solution in the case where the potential takes the form $U(x) = \lambda \, \mathrm{sn}^2(x,k)$. In the other two cases, the solutions degenerate to that previously given for the sech^2 potential.

F. Harmonic potential

Next, we may examine the harmonic oscillator potential $U(x) = \lambda x^2$ with $\lambda \in \mathbb{R}$. Harmonic potentials have been used as external potentials for BECs in a number of studies, as they serve as a relatively accurate and simple model of a parabolic trap [20]. It should be noted that such potentials can be generalized to include time dependence [21], but this is beyond the scope of this paper as such generalizations can deny us of a stationary state of the kind we study here.

In this case, $\psi_0(x)$ is given in Eq. (14). Let us define the functions

$$M_1(x) = 36(e^{2x} + 1)^2[\mathrm{Li}_2(-e^{2x}) + 2x\ln(e^{2x} + 1)]$$
$$- (8x^3 + 72x^2 - 3\pi^2)e^{4x}$$
$$+ (128x^3 - 72x^2 + 6\pi^2)e^{2x} - 8x^3 + 3\pi^2 \quad (41)$$

and

$$M_2(x) = (e^{2x} + 1)^2 \ln(e^{2x} + 1) - (\ln 2 - 2x)e^{4x}$$
$$+ (2x^2 - 2x - 2\ln 2)e^{2x} - \ln 2, \qquad (42)$$

so that the first-order term $\psi_1(x)$ reads as

$$\psi_1(x) = \frac{\lambda}{48(1 + e^{2x})^2}\{\mathrm{sech}(x)\tanh(x)M_1(x) - 24[\cosh(x)$$
$$+ 3x\,\mathrm{sech}(x)\tanh(x) - 3\,\mathrm{sech}(x)]M_2(x)\}. \qquad (43)$$

Note that the polylogarithm $\mathrm{Li}_s(z)$ is a special function defined by the infinite sum

$$\mathrm{Li}_s(z) = \sum_{k=1}^{\infty} \frac{z^k}{k^s},$$

also known as the Bose-Einstein integral in quantum statistics for its representation as the closed form of integrals of the
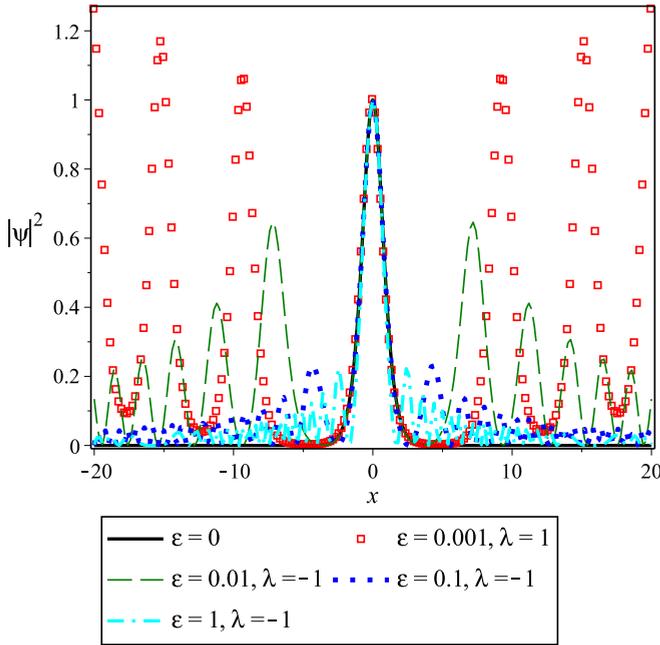
FIG. 1. (Color online) Perturbations of the bright soliton solution under the harmonic oscillator potential, which takes the quadratic form $U(x) = \lambda x^2$, on $-20 \leqslant x \leqslant 20$. Solutions corresponding to $\lambda < 0$ exhibit oscillations that gradually decay in the density $|\psi|^2$ as $|x|$ becomes large. As ϵ is increased, the rate of decay of the average density is increased. In the case where $\lambda > 0$, the solutions exhibit oscillations which gradually increase in intensity. The width of each density peak appears to decrease to counter these spikes. If the domain was unbounded, these excitations would likely lead to instability. All solutions corresponding to $\epsilon \leqslant 0.1$ are perturbation solutions, while for $\epsilon = 1$ we use numerical solutions.

Bose-Einstein distribution, namely,

$$\mathrm{Li}_s(z) = \frac{1}{\Gamma(s)} \int_0^\infty \frac{t^{s-1}}{e^t/z - 1} \, dt,$$

where $\Gamma(\mu) = \int_0^\infty t^{\mu-1} e^{-t} \, dt$.

In Fig. 1, we demonstrate some of these solutions for various ϵ and λ. Solutions corresponding to $\lambda < 0$ exhibit oscillations that gradually decay in the density $|\psi|^2$ as $|x|$ becomes large. As ϵ is increased, the rate of decay of the average density is increased. In this case, the increase in ϵ results in most of the mass clustered near the origin, so the solution profiles actually are rather close to the bright soliton in the large epsilon limit, which might be counterintuitive. In the large ϵ limit, the greatest agreement with the perturbation solutions and the bright soliton is in the tails of such solutions, where the density decays rapidly. On the other hand, for small ϵ, we note that the solutions are in excellent agreement with the bright solitons near the origin, while such solutions have larger density peaks for intermediate values of $|x|$. We suspect that this is caused by the fact that general solutions can be given in the form of $\psi(x) = A \operatorname{sn}(\nu x, k)$. When $k \to \pm 1$, solutions of this kind degenerate into the form $\psi(x) = A \operatorname{sech}(\nu x)$ (a nonperiodic soliton). However, for k near but not equal to ± 1, we have space-periodic solutions. So, the perturbations here can be viewed as perturbations of the Jacobi elliptic

index k, and as a result, small ϵ perturbations acting on a bright soliton $\psi(x) = A \operatorname{sech}(\nu x)$ can result in space-periodic solutions, no matter how small the perturbations are. In that sense, it appears as though the bright solitons are unstable under small ϵ perturbations. It is interesting that, for large ϵ, we see the solutions return to the form of a bright soliton, with only minor corrections to the density profiles.

In the case where $\lambda > 0$, the solutions exhibit oscillations which gradually increase in intensity. The width of each density peak appears to decrease to counter these spikes. It is likely that such solutions are unstable. So, for $\lambda < 0$ the small potential permits oscillations which are damped and gradually decay to zero (as would be expected if one were to perturb a pure bright soliton) while perturbations in the potential corresponding to $\lambda > 0$ result in oscillations in the density which grow as one moves away from the origin. In the case where one is confined to a finite interval, say $-\ell \leqslant x \leqslant \ell$, this means that when $\lambda < 0$ the confining potential forces the greatest density to occur near the origin. On the other hand, when $\lambda > 0$, the density is spread out over the domain in multiple density peaks.

Note that for small ϵ the perturbation solutions can be used, while for larger ϵ (such as $\epsilon = 1$) numerical simulations were used.

G. Modified harmonic potential

There have been a number of modifications to the harmonic trap used in the literature [22]. One such potential is $U(x) = \lambda(x^2 + \beta/x^\alpha)$. Another useful potential is $U(x) = \lambda[x^2 + \beta \exp(-x^2)]$. This latter potential is useful in that it avoids a singularity near the origin.

We consider solutions for the potential $U(x) = \lambda[x^2 + \beta \exp(-x^2)]$, and plot the perturbations of the bright soliton in Fig. 2. For the case where $\lambda < 0$, the results are similar to that of the previous example. Most of the mass is allocated near the origin (with decay in the density plots as $|x|$ becomes large), and as ϵ is increased, the rate of decay of the additional density peaks increases.

In the case where $\lambda > 0$, there appears to be positive mass over a large region once one is far enough away from the origin. The density plot still shows oscillations, but these increase along what appears to be a linear trend as one moves away from $x = 0$. So, when we have a symmetric interval $-\ell \leqslant x \leqslant \ell$, the $\lambda > 0$ case has much of the density allocated away from the origin, while in the $\lambda < 0$ case most of the density is near the origin.

What we see again is that when the potential is positive, much of the mass is allocated throughout the problem domain (including away from the origin), while when the potential is negative, the mass is trapped near the origin. The strength of the trap corresponds to the size of ϵ, so for small ϵ these effects are minor, while for large ϵ the trap is much stronger.

H. An asymmetric trap

Single-well traps that are asymmetric are sometimes considered, and can take a variety of forms. The Morse potential is one example of an asymmetric trap [23,24]. The Morse potential is given by $U(x) = \lambda(e^{-2Ax} - 2e^{-Ax})$ where $\lambda > 0$
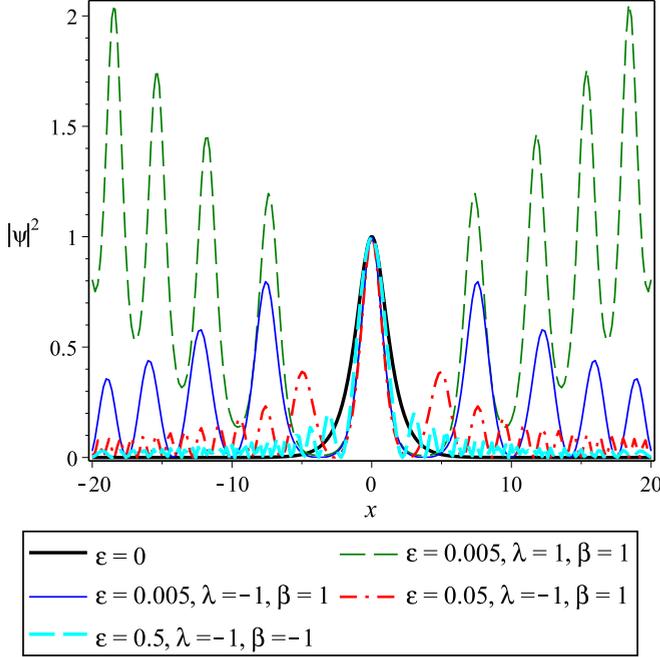
FIG. 2. (Color online) Perturbations of the bright soliton solution under the modified harmonic oscillator potential $U(x) = \lambda[x^2 + \beta \exp(-x^2)]$, on $-20 \leqslant x \leqslant 20$. Solutions corresponding to $\lambda < 0$ exhibit oscillations that gradually decay in the density $|\psi|^2$ as $|x|$ becomes large. For larger ϵ, the trap potential is stringer, and hence more of the mass is allocated near the origin. In the case where $\lambda > 0$, the solutions exhibit oscillations which gradually increase in intensity. Such excitations also increase in an average sense, with the oscillations themselves increasing along a linear trend. The width of each density peak appears to be smaller in the $\lambda > 0$ case than in the $\lambda < 0$ case, likely due to the fact that mass is allocated over a larger region. All solutions corresponding to $\epsilon \leqslant 0.05$ are perturbation solutions, while for $\epsilon = 0.5$ we use numerical solutions.

and $A > 0$. In contrast to the harmonic trap, the Morse potential increases more slowly along the positive x axis. In relation to BECs, the Morse potential has previously been considered for models of trapped atoms [25].

We consider the Morse potential and plot perturbations of the bright soliton solution in Fig. 3. In the case where $\lambda > 0$, the density plots oscillate on one half of the interval considered. The side on which they oscillate depends on the sign of A: if $A > 0$, the oscillations occur on $x > 0$, while when $A < 0$ the oscillations occur for $x < 0$. The solutions rapidly grow and become nonphysical on the other side of the origin. This may imply that such solutions are unstable in the $\lambda > 0$ regime.

In the $\lambda < 0$ regime, solutions oscillate in density on one half of the domain, and then decay on the other half. Again, the location of the oscillations is tied to the sign of A. If $A < 0$, the the oscillations will be found on $x < 0$ and the solutions decay rapidly for $x > 0$. On the other hand, if $A > 0$, the density oscillates on $x > 0$, and decays rapidly as $x < 0$. These results make sense. Indeed, as the Morse potential is an asymmetric trap, it skews the mass to one side of the origin. The sign of A can then be used to control the way in which the density shifts.
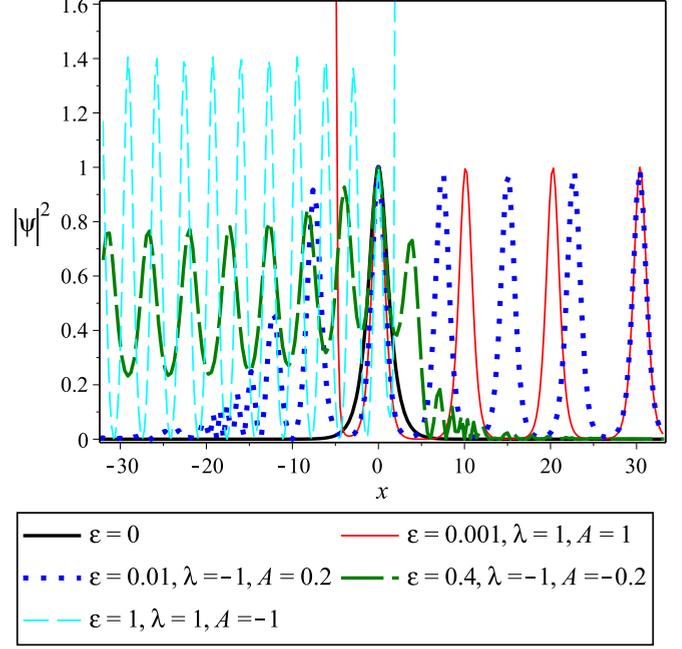

FIG. 3. (Color online) Perturbations of the bright soliton solution under the Morse potential $U(x) = \lambda(e^{-2Ax} - 2e^{-Ax})$ on the symmetric interval $-33 \leqslant x \leqslant 33$. Since the Morse potential is an asymmetric trap, the perturbations due to small-magnitude Morse potentials will force the mass of the perturbed bright soliton to be allocated to one side of the origin $x = 0$, with decay occurring on the other side (when $\lambda < 0$). The sign of A determines the form of the asymmetry. All solutions corresponding to $\epsilon \leqslant 0.1$ are perturbation solutions, while for $\epsilon = 0.4$ and $\epsilon = 1$ we use numerical solutions.

I. Quantum pendulum potential: A lattice trap

The quantum pendulum potential takes the form $U(x) = \lambda[1 - \cos(x)]$. This is a good model of an optical lattice type of potential, which has been used to study BECs in a number of settings [26]. $\psi_0(x)$ again remains as given in Eq. (14), but $U(x) = \lambda[1 - \cos(x)]$ results in a first-order perturbation term $\psi_1(x)$ of the form

$$
\psi_1(x) = \frac{\lambda}{4}[\cosh(x) + 3x\,\mathrm{sech}(x)\tanh(x) - 3\,\mathrm{sech}(x)]
$$
$$
\times \left\{1 - \mathrm{sech}^2(x) - \int_0^x \mathrm{sech}^2(y)\tanh(y)\cos(y)\,dy\right\}
$$
$$
- \frac{\lambda}{2}\mathrm{sech}(x)\tanh(x)
$$
$$
\times \left\{x - \frac{3(4xe^{2x} - e^{4x} + 1)}{2(e^{2x} + 1)^2} - 3\tanh(x) - \sin(x)\right.
$$
$$
\left. + 3\int_0^x \cos(y)\mathrm{sech}^2(y)[1 - y\tanh(y)]\,dy\right\}. \quad (44)
$$

In Fig. 4, we plot the density $|\psi|^2$ over the symmetric interval $-30 \leqslant x \leqslant 30$ for the lattice trap $U(x) = \lambda[1 - \cos(x)]$. In the case of $\lambda < 0$, the primary density peak occurs at the origin, while additional density peaks are observed. The appearance of such additional peaks is somewhat regular, although the height of such peaks is not. Unlike in previous cases, where
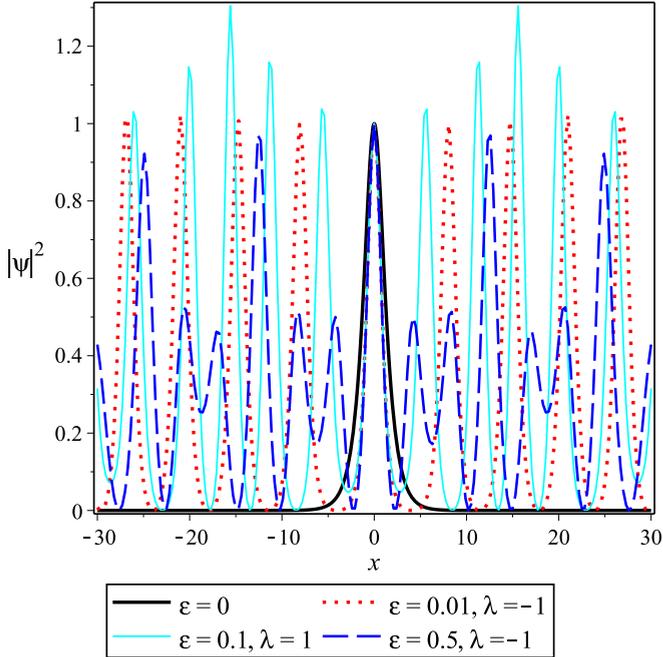
FIG. 4. (Color online) Perturbations of the bright soliton solution under the lattice potential $U(x) = \lambda\,[1 - \cos(x)]$ on the symmetric interval $-30 \leqslant x \leqslant 30$. For both $\lambda > 0$ and $\lambda < 0$, the density remains bounded and exhibits oscillations. Unlike the previous cases considered, these oscillations are not damped for any sign of λ. For $\lambda > 0$, the maximum density is allocated away from the origin (although a local maxima does occur at the origin). In contrast when $\lambda < 0$, the maximal density occurs at the origin, with many smaller local maxima occurring away from the origin. The lattice trap is space periodic, so it permits a positive density maxima arbitrarily far from the origin. All solutions corresponding to $\epsilon \leqslant 0.1$ are perturbation solutions, while for $\epsilon = 0.5$ we use numerical solutions.

the peaks gradually decayed, we observe a decrease, then an increase, and so on.

For $\lambda > 0$, we observe a similar structure, with the difference being that the density peak at the origin is smaller than surrounding density maxima. So, when $\lambda < 0$, the potential traps a large amount of the mass near the origin, while other local maxima still occur. On the other hand, $\lambda > 0$ gives a trap that allocates much more of the mass away from the origin.

For both $\lambda > 0$ and $\lambda < 0$, we have bounded persistence of the density far from the origin. This is due to the fact that the potential is bounded and periodic, which allows accumulations of mass to congregate even far from the origin.

J. Double-well potential

Various applications call for double-well potentials [27]. One possible form of such a potential used is $U(x) = \lambda[(x^2 - 1)^2 - \beta]$, which gives a simple and symmetric double well. One may use the formulas in Sec. III to obtain the first-order perturbation solution corresponding to a double-well potential. We omit the details here, and summarize the results. We consider the potential $U(x) = U(x) = \lambda[(x^2 - 1)^2 - \beta]$, and plot the perturbations of the bright soliton in Fig. 5 on the interval $-6 \leqslant x \leqslant 6$.
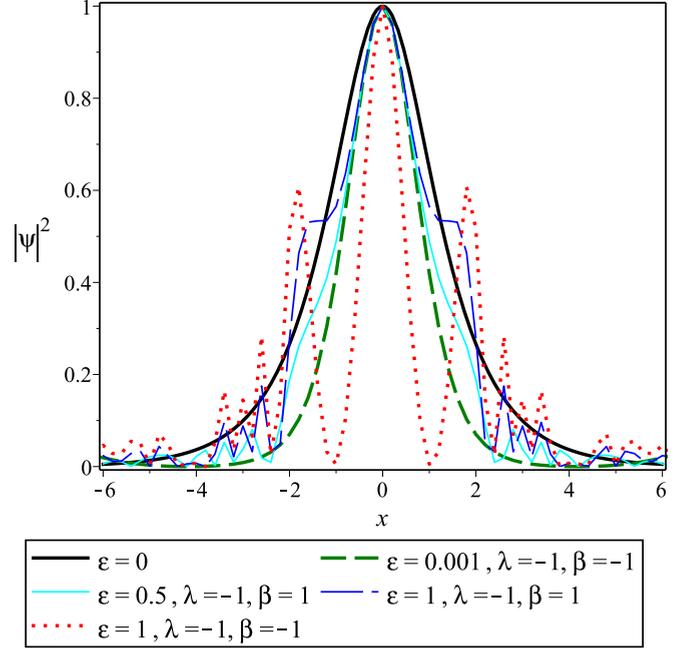

FIG. 5. (Color online) Perturbations of the bright soliton solution under the double-well potential $U(x) = \lambda[(x^2 - 1)^2 - \beta]$ on $-6 \leqslant x \leqslant 6$. The potential acts as a confining potential for $\lambda < 0$ and appears to induce an instability when $\lambda > 0$. Indeed, the $\lambda < 0$ potential is a rather effective confining potential, as the density plots show that the mass is confined to near the origin for both large and small ϵ. All solutions corresponding to $\epsilon \leqslant 0.1$ are perturbation solutions, while for $\epsilon = 0.5$ and 1 we use numerical solutions.

In all of the cases considered here, we have considered $\lambda < 0$. The $\lambda > 0$ case is seemingly unstable, denoting blowup of the solutions (hence mass is not conserved). In the $\lambda < 0$ case, we have a confining potential, and we see that for all ϵ considered that the solutions are rather close in form to the bright soliton solution.

The perturbations exhibit oscillations which decay (and which are contained in an envelope which approximates the bright soliton) for large enough ϵ, no matter the sign of β. In this case, most of the mass is allocated near the origin (as is true of the pure bright soliton solution). As ϵ is made small, the period of these oscillations tends to increase, with less mass allocated near the origin.

K. Harmonic potential with lattice trap

It is possible to combine a harmonic potential and lattice trap, or another combination of traps, to obtain pseudoperiodic or quasiperiodic potentials, and this type of potential has been considered previously in differing settings [28]. One possible form of such a potential is $U(x) = \lambda[x^2 + \beta\cos^2(x)]$, which was used in Ref. [29]. This class of potential was shown to be useful for studying the one-dimensional (1D) dynamics of a BEC of cold atoms in parabolic optical lattices [30]. We shall present some graphical results, but shall omit the detailed derivation of the perturbation solutions. Note that perturbation results can be obtained for a number of different types of lattice traps. We consider the potential
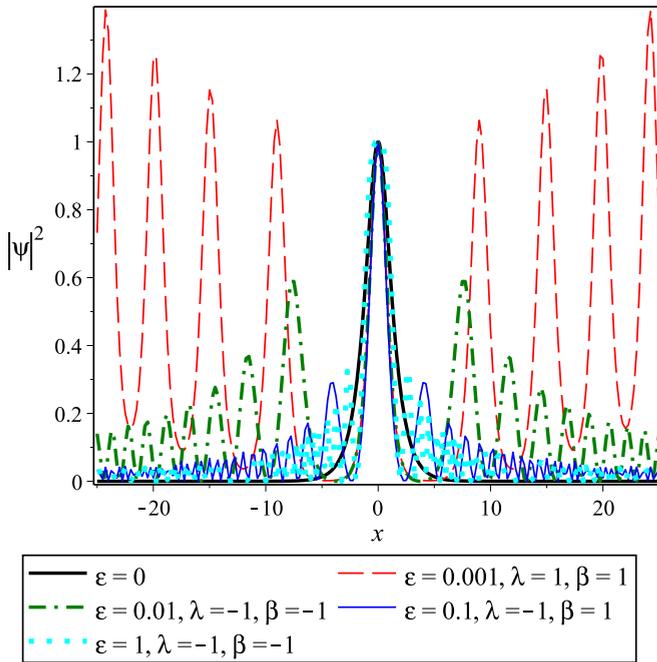
FIG. 6. (Color online) Perturbations of the bright soliton solution under the modified harmonic oscillator potential $U(x) = \lambda[x^2 + \beta \cos^2(x)]$ on $-25 \leqslant x \leqslant 25$. When $\lambda < 0$, the potential acts as a trap, confining most of the mass to near the origin. When $\lambda > 0$, the opposite is true, and we see that the mass (in an average sense) increases as one approaches the boundary of the domain. All solutions corresponding to $\epsilon \leqslant 0.1$ are perturbation solutions, while for $\epsilon = 1$ we use numerical solutions.

$U(x) = \lambda[x^2 + \beta \cos^2(x)]$ since this potential is reasonably simple and has been considered elsewhere.

In Fig. 6, we plot the density $|\psi|^2$ for the perturbations of the bright solitons given a potential of the form $U(x) = \lambda[x^2 + \beta \cos^2(x)]$. Here, we take the symmetric interval $-25 \leqslant x \leqslant 25$. The results are similar to those of the modified harmonic potential (shown in Fig. 2). In the case where $\lambda < 0$, most of the mass is confined to the region near the origin, so the density max is at $x = 0$. There are secondary local maxima symmetric on either side of the origin. The larger the value of ϵ, the smaller these secondary maxima become.

When $\lambda > 0$, the potential is no longer trapping the mass, and hence there exist density maxima throughout the domain. As one moves away from $x = 0$, these maxima increase in value, so the smallest density maxima occur at the origin.

V. CONCLUSIONS

We have obtained the general perturbation theory for the cubic NLS with small potentials in the case of an attractive nonlinearity. This equation governs an attractive BEC in $1 + 1$ dimensions. The primary benefit to our approach is that we were able to account for general potential functions. The approach involves perturbation around a bright soliton (the stationary state for the potential zero BEC). Another benefit to the method employed is that we did not have to assume a small unperturbed solution. Rather, the unperturbed solution can be

of any size since only the perturbation corrections should be sufficiently small.

There are a number of varieties of potentials which permit exact solutions for the attractive BECs. Most of these are in the form of some scaling of the bright soliton. In such cases, the addition of the small potential causes no strong qualitative change in the solutions. For other potentials, such as the δ potential, the bright soliton solution degenerates into a space-periodic solution in part of the domain. In such a case, there is still a density maxima at $x = 0$, although other maxima also occur.

For more complicated potentials (such as those commonly found in the study of BECs), the perturbation results are useful. Often, the perturbations of the bright solitons due to these small potentials have one of two effects. If the small potential is negative, it acts as a confining potential. In this scenario, most of the density is allocated near the origin, although there can be smaller local density maxima away from the origin. These small excitations gradually decay as one moves away from the origin. On the other hand, when the potential is positive, it forces the density to spread out over a symmetric domain $-\ell \leqslant x \leqslant \ell$. In the case of asymmetric potentials, the density can be allocated to one side of this symmetric interval.

In obtaining the solutions displayed in Sec. IV, note that perturbation solutions were obtained for sufficiently small ϵ, while for larger values of ϵ numerical solutions are provided. For small enough ϵ, there is excellent agreement between the analytical perturbation results and the numerical solutions. As ϵ increases in value, the perturbation solutions gradually lose accuracy. We demonstrate this in Fig. 7, where we compare the perturbation results with the numerical solutions for the lattice potential corresponding to $U(x) = 1 - \cos(x)$. The breakdown of the perturbation results as ϵ increases results in a loss of agreement away from the origin, while the solutions remain reasonably accurate near the origin. This means that, for larger ϵ, the perturbation solutions lose accuracy when the solution oscillates. The reason for this is that for larger ϵ, the period of oscillation is poorly approximated. In order to more accurately capture the oscillatory nature of these solutions, it is possible that a multiple-scales analysis would prove useful. Similarly, in Fig. 8, we give a similar plot for numerical and perturbation solutions in the case of the Morse potential. That the perturbation and numerical results agree in the small ϵ regime makes sense, as when ϵ is sufficiently small, the perturbation solution is essentially going to converge in a geometric manner (in powers of this small ϵ). This manner of convergence can not be expected to hold when ϵ is not small, as nonlinear effects tend to amplify the correction terms. This is why we resort to numerical solutions in the cases where ϵ is not small enough.

One requirement in the method employed is that the potential function be piecewise continuous. When a potential does not satisfy such a condition, the perturbation method breaks down. Such an example would be a potential of the type λ/x^α. When $\alpha > 2$, the solution to the NLS can develop a nonremovable singularity at the origin. In such a case, one should consider a nonlocal formulation of the model (as was used in the original derivation of the GP equation).

In the case of more than one spatial dimension, the stationary solution is determined by a solution to
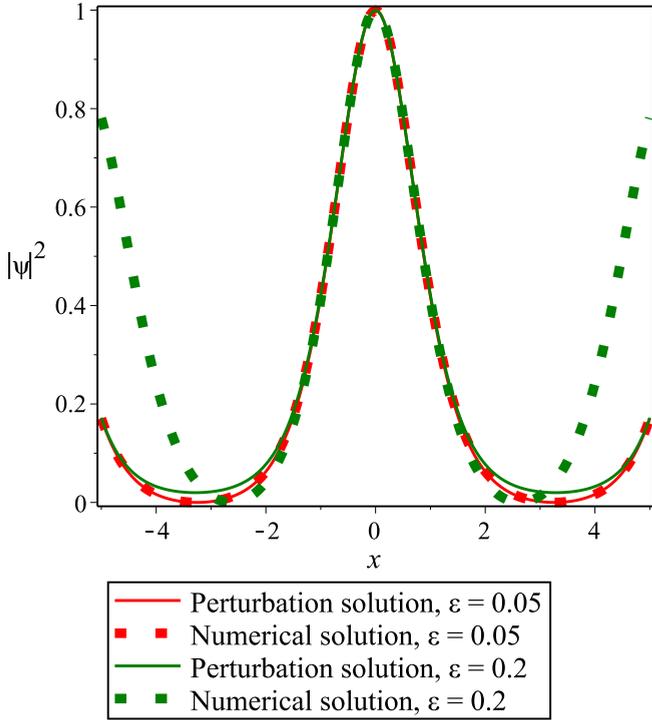
FIG. 7. (Color online) Perturbations of the bright soliton solution under the lattice potential corresponding to $U(x) = 1 - \cos(x)$ on the symmetric interval $-5 \leqslant x \leqslant 5$. We see that for small enough ϵ, the perturbation and numerical solutions agree very well, as seen in the lower of the curves plotted. Once ϵ becomes larger, the solution is no longer in the perturbative regime, and therefore the perturbation solutions break down (as seen when $\epsilon = 0.2$), which is shown in the upper dotted curve. For all solutions, the agreement is still very good close to $x = 0$, with the breakdown occurring for larger values of x.
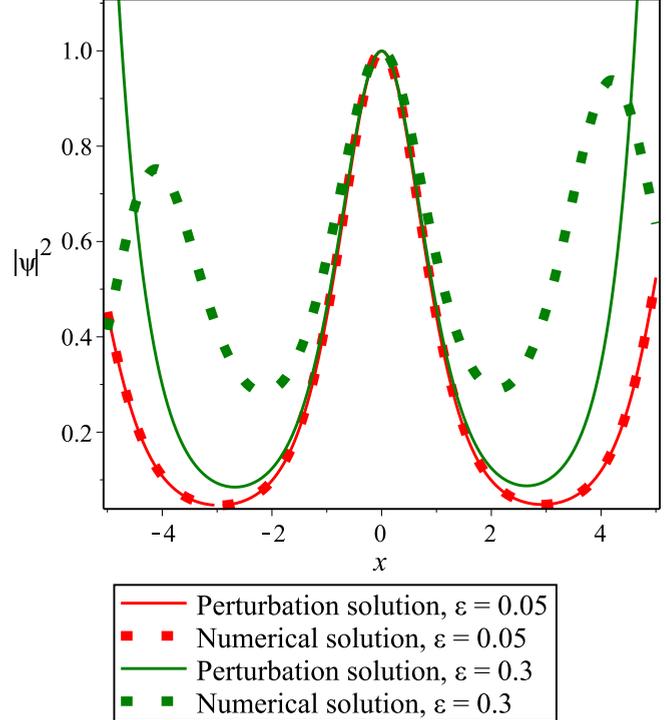

FIG. 8. (Color online) Perturbations of the bright soliton solution under the Morse potential corresponding to $U(x) = -(e^{-0.4x} - 2e^{-0.2x})$ on the symmetric interval $-5 \leqslant x \leqslant 5$. Again, for small enough ϵ, the perturbation and numerical solutions agree very well (such as in the case of $\epsilon = 0.05$) since the lower dotted and solid curves coincide. For larger ϵ (such as $\epsilon = 0.3$), the agreement between the numerical and perturbation solutions break down, owing to the fact that the perturbation solutions are valid in the small ϵ regime. We see this from the fact that the upper solid and dotted curves do not coincide, unless x is small. For all solutions, the agreement is still very good close to $x = 0$, with the breakdown occurring for larger values of x.

the PDE

$$\triangle \psi + [1 - \epsilon U(\mathbf{x})]\psi - 2\psi^3 = 0. \tag{45}$$

If one can obtain a solution to the $\epsilon = 0$ nonlinear equation $\triangle \psi + \psi - 2\psi^3 = 0$, then the perturbation method discussed here can be applied. If one assumes radial symmetry, then the wave function can be given in terms of $\psi(x_1, \ldots, x_N) = \psi(r)$, where

$$\psi''(r) + \frac{N-1}{r}\psi'(r) + [1 - \epsilon U(r)]\psi(r) - 2\psi(r)^3 = 0, \tag{46}$$

where we also assume a radially symmetric potential function. Unlike in the case of the bright soliton perturbation theory considered here (or in the case of the dark soliton perturbation theory discussed in Ref. [15]), the $\epsilon = 0$ reduction of this model does not have an exact solution. So, one would likely be required to consider small amplitude solutions. A multiple scales approach could prove useful. This will be taken up in future work.

The stability or instability of stationary states for various integrable models can be determined through an application of the Vakhitov-Kolokolov (VK) stability criteria [31]. Recently, the stability of these types of solutions has been considered for other integrable models admitting sn-wave or cn-wave solutions, such as the integrable Wadati-Konno-Ichikawa-Shimizu [32] and local induction approximation [33] models. The present solutions belong to the cn-wave family (since in the limit where the Jacobi elliptic index goes to one, the cn function reduces to the sech solution), so a stability analysis for perturbation of cn waves due to small potentials would be of interest. While perturbation results were obtained for various potentials, stability results may be more dependent on the exact type of potential studied.

[1] F. Dalfovo, S. Giorgini, L. P. Pitaevskii, and S. Stringari, Rev. Mod. Phys. **71**, 463 (1999); L. D. Carr, M. A. Leung, and W. P. Reinhardt, J. Phys. B: At., Mol. Opt. Phys. **33**, 3983 (2000); M. Key, I. G. Hughes, W. Rooijakkers, B. E. Sauer, E. A. Hinds, D. J. Richardson, and P. G. Kazansky, Phys. Rev. Lett. **84**, 1371 (2000); N. H. Dekker, C. S. Lee, V. Lorent, J. H. Thywissen, S. P. Smith, M. Drindic, R. M. Westervelt, and M. Prentiss, *ibid.* **84**, 1124 (2000).

[2] M. Kunze *et al.*, Phys. D (Amsterdam) **128**, 273 (1999); Y. S. Kivshar, T. J. Alexander, and S. K. Turitsyn, Phys. Lett. A **278**, 225 (2001).

[3] S. Theodorakis and E. Leontidis, J. Phys. A **30**, 4835 (1997); F. Barra, P. Gaspard, and S. Rica, Phys. Rev. E **61**, 5852 (2000).

[4] J. C. Bronski, L. D. Carr, B. Deconinck, and J. N. Kutz, Phys. Rev. Lett. **86**, 1402 (2001).

[5] B. P. Anderson and M. A. Kasevich, Science **282**, 1686 (1998); E. W. Hagley *et al.*, *ibid.* **283**, 1706 (1999).

[6] Y. B. Ovchinnikov, J. H. Muller, M. R. Doery, E. J. D. Vredenbregt, K. Helmerson, S. L. Rolston, and W. D. Phillips, Phys. Rev. Lett. **83**, 284 (1999).

[7] D. Jaksch, C. Bruder, J. I. Cirac, C. W. Gardiner, and P. Zoller, Phys. Rev. Lett. **81**, 3108 (1998); G. K. Brennen, C. M. Caves, P. S. Jessen, and I. H. Deutsch, *ibid.* **82**, 1060 (1999).

[8] D.-I. Choi and Q. Niu, Phys. Rev. Lett. **82**, 2022 (1999).

[9] L. D. Carr, C. W. Clark, and W. P. Reinhardt, Phys. Rev. A **62**, 063610 (2000).

[10] L. D. Carr, C. W. Clark, and W. P. Reinhardt, Phys. Rev. A **62**, 063611 (2000).

[11] X.-F. Zhou, S.-L. Zhang, Z.-W. Zhou, B. A. Malomed, and H. Pu, Phys. Rev. A **85**, 023603 (2012).

[12] H. Cartarius and G. Wunner, Phys. Rev. A **86**, 013612 (2012).

[13] R. D'Agosta and C. Presilla, Phys. Rev. A **65**, 043609 (2002).

[14] E. M. Lifshitz and L. P. Pitaevskii, *Statistical Physics Part 2: Landau and Lifshitz Course of Theoretical Physics* (Butterworth-Heinemann, London, 1980).

[15] K. Mallory and R. A. Van Gorder, Phys. Rev. E **88**, 013205 (2013).

[16] R. A. Van Gorder, J. Fluid Mech. **707**, 585 (2012); Prog. Theor. Phys. **128**, 993 (2012); Phys. Rev. E **86**, 057301 (2012).

[17] R.-J. Lange, J. High Energy Phys. 11 (2012) 032.

[18] W. van Dijk and K. A. Kiers, Am. J. Phys. **60**, 520 (1992); T. C. Scott, J. F. Babb, A. Dalgarno, and J. D. Morgan, III, J. Chem. Phys. **99**, 2841 (1993).

[19] N. Regnault and T. Jolicoeur, Phys. Rev. Lett. **91**, 030402 (2003).

[20] Z. X. Liang, Z. D. Zhang, and W. M. Liu, Phys. Rev. Lett. **94**, 050402 (2005); S. K. Adhikari, Phys. Rev. E **62**, 2937 (2000); V. M. Pérez-García, H. Michinel, J. I. Cirac, M. Lewenstein, and P. Zoller, Phys. Rev. A **56**, 1424 (1997); W. Bao, D. Jaksch, and P. A. Markowich, J. Comput. Phys. **187**, 318 (2003).

[21] G. Theocharis, Z. Rapti, P. G. Kevrekidis, D. J. Frantzeskakis, and V. V. Konotop, Phys. Rev. A **67**, 063610 (2003).

[22] M. Landtman, Phys. Lett. A **175**, 147 (1993); A. L. Fetter, Phys. Rev. A **64**, 063608 (2001).

[23] P. M. Morse, Phys. Rev. **34**, 57 (1929).

[24] Y. Zhou, M. Karplus, K. D. Ball, and R. S. Bery, J. Chem. Phys. **116**, 2323 (2002).

[25] W. C. Stwalley and L. H. Nosanow, Phys. Rev. Lett. **36**, 910 (1976); B. D. Esry and C. H. Greene, Phys. Rev. A **60**, 1451 (1999).

[26] S. Burger, F. S. Cataliotti, C. Fort, F. Minardi, M. Inguscio, M. L. Chiofalo, and M. P. Tosi, Phys. Rev. Lett. **86**, 4447 (2001); M. Greiner, I. Bloch, O. Mandel, T. W. Hänsch, and T. Esslinger, *ibid.* **87**, 160405 (2001); M. Greiner, O. Mandel, T. W. Hänsch, and I. Bloch, Nature (London) **419**, 51 (2002); C. Orzel, A. K. Tuchman, M. L. Fenselau, M. Yasuda, and M. A. Kasevich, Science **291**, 2386 (2001); G. Chong, W. Hai, and Q. Xie, Phys. Rev. E **70**, 036213 (2004).

[27] G. J. Milburn, J. Corney, E. M. Wright, and D. F. Walls, Phys. Rev. A **55**, 4318 (1997); Y. Shin, M. Saba, T. A. Pasquini, W. Ketterle, D. E. Pritchard, and A. E. Leanhardt, Phys. Rev. Lett. **92**, 050405 (2004); A. Smerzi, S. Fantoni, S. Giovanazzi, and S. R. Shenoy, *ibid.* **79**, 4950 (1997); L. Pitaevskii and S. Stringari, *ibid.* **87**, 180402 (2001); J. Ruostekoski and D. F. Walls, Phys. Rev. A **58**, R50 (1998); R. W. Spekkens and J. E. Sipe, *ibid.* **59**, 3868 (1999); K. W. Mahmud, H. Perry, and W. P. Reinhardt, *ibid.* **71**, 023615 (2005).

[28] G. Roati *et al.*, Nature (London) **453**, 895 (2005); F. S. Cataliotti, L. Fallani, F. Ferlaino, C. Fort, P. Maddaloni, and M. Inguscio, New J. Phys. **5**, 71 (2003); A. Smerzi and A. Trombettoni, Phys. Rev. A **68**, 023613 (2003); K. J. H. Law, P. G. Kevrekidis, B. P. Anderson, R. Carretero-González, and D. J. Frantzeskakis, J. Phys. B: At., Mol. Opt. Phys. **41**, 195303 (2008).

[29] L. Fallani, L. De Sarlo, J. E. Lye, M. Modugno, R. Saers, C. Fort, and M. Inguscio, Phys. Rev. Lett. **93**, 140406 (2004).

[30] J. Brand and A. R. Kolovsky, Eur. Phys. J. D **41**, 331 (2007).

[31] N. G. Vakhitov and A. A. Kolokolov, Izv. Vyssh. Uchebn. Zaved., Radiofiz. **16**, 1020 (1973) [Sov. Radiophys. **16**, 783 (1973)].

[32] R. A. Van Gorder, J. Phys. Soc. Jpn. **82**, 064005 (2013).

[33] R. A. Van Gorder, J. Phys. Soc. Jpn. **82**, 094005 (2013).